Al-Qadisiyah Journal of Pure Science

Volume 29 | Number 2 Article 20

12-20-2024

A Study of Unstable MHD Free Convection over a Vertical Plate in a Two Dimensions under the Influence of Radiation

Alaa A. Hammodat
College of Education for Pure Science/University of Mosul, alaa.hammodat@gmail.com

Iman Al-Obaidi

Ghanim M. Algwauish

ORIGINAL STUDY

A Study of Unstable MHD Free Convection Over a Vertical Plate in a Two Dimensions Under the Influence of Radiation

Alaa A. Hammodat*, Iman Al-Obaidi, Ghanim M. Algwauish

University of Mosul, Iraq

Abstract

This research studies the case of unsteady heat flux under the influence of two main factors: thermal radiation and magnetic force across a vertical plate. In order to explore the partial differential equations without introducing the dimensions of energy, momentum and continuity, a set of dimensionless nonlinear systems of partial differential equations were solved using the numerical finite difference method. Because of the assumed parameter ramifications of the velocity and temperature problem are also investigated without dependence on dimensions. Temperatures and momentum profiles are derived via finite differences. Following that, a qualitative and visual presentation of the parameter results on the velocity and temperature profiles is made.

Keywords: Heat transfer flow, Unsteady state equations, Magnetic field, Finite difference method

1. Introduction

The focus of the field of study known as magneto hydrodynamics (MHD) involves reviewing and examining electrically conductive motion in fluids under the influence of a magnetic field. One of these fluids is plasma, which is made up of ionized gases like those found in the solar atmosphere and liquid metals (like molten iron and mercury). A well-known application of the MHD principle is the dynamo and motor. In a vertical channel, numerous studies have been conducted on the unsteady MHD free convective flows. The basis for these scientific investigations is the fact that research into such flows has a wide range of scientifically motivating applications in numerous fields. MHD power generators, MHD pumps, liquid metal cooling of reactors, magnetic drug targeting, etc. are some of these applications. Various studies have contributed to this field [1]. The varying mass and heat transfer as well as the unsteady MHD free flow as a fluid radiates and reacts beyond a vertical porous evaluated plate were identified by Kumar S. and Singh Ch. in 2009 [2]. The scientist Seethamahalakshmi and others investigated MHD free irregular convection and flow near a moving top plate in 2011 [3].

In 2013, Zhang et al. dealt with and studied the effects of walls on heat transfer and fluid influx using MHD with distinct Pi numbers and Hartmann numbers [4]. In order to study the unstable mixed convection, Narahari M. et al. used an accelerating vertical sheet with a continuous thermal gradient and a heat source in 2014 [5]. The numerical calculations of the friction coefficient of skin and local Nusselt for the matter of flow at the point of stagnation for a Casson fluid and heat transfer on a stretching/shrinking plate in a non-porous channel were discussed by Namdeppanavar M. and Shilpa J. in 2016 [6].

A non-uniformly permeable material with varying permeability that is surrounded by an unbounded porous vertical surface was the subject of an analytical investigation by Ibrahim M. and Suneetha K [7]. In 2017, Kumari K. and Goyal M. took a porous channel with uneven walls and studied the effect of transverse magnetic field and radiative

Received 28 March 2023; accepted 30 June 2023.
Available online 18 April 2025

* Corresponding author.
E-mail address: alaahammodat@uomosul.edu.iq (A.A. Hammodat).

https://doi.org/10.29350/2411-3514.1300

heat transfer on the irregular flow of an optical conductive fluid. The results showed that while the wall shear stress decreased with increasing magnetic field strength, it increased with increasing radiation parameters [8]. In order to understand how Soret-Dufour, radioactivity, through sloping porous sheet embedded in a permeable medium, the chemical bonding influences the non-uniform MHD flow of the contaminated liquid. Pandya N. and Yadav R. conducted research [9]. In the same year, Al-Amin et al. to know the influence of the magnetic field on fluid, we using the simulation to investigate by a single-phase warmness transport in the pored diversity in 2018 [10] and took the variation in Nanofluid concentration into consideration. In 2019, Rahman A. et al. dissected the airflow in an MHD system in a rectangular channel and looked at the process for assessing a channel's flow stability [11].

To solve the computational issue of fluid heat transfer through diffusion and radiation in a rectangular layer while being impacted by an electromagnetic field (EMF) by 2021, Hammodat A. and et al. used the alternative directed implicit technique (ADI) [12]. Sharif Ullah et al. carried out a thorough examination of the unstable over a vertical channel, MHD rid convection outpour same year. We use a finite difference approach to directly solve the issues [13]. Using a chemical reaction, a magnetic force, and a Soret alignment, Nagaraju V. et al. studied the unsteady fluid-dynamic flow over a sloped plate in a porous medium in 2021 [14]. Joel C. and Adeshina T. explain how variable conductivity in 2022 will affect the thermal stability of an exergonic reactionary fluid in dynamic flow through parallel plates [15].

In the same year [16], Bodoloi R. and Ahmed N. created an analytical method for the problem of and double unstable free convective MHD mass transfer flow pattern of viscosity, immiscible, spectrally fine the liquid above the medium upright permeable plate. The direct purpose of this research is to investigate MHD free convection flows along a perpendicular character under the actuality of a magnetic domain and heat flux. The distributions of temperature and velocity for a viscosity, incompressible fluid flowing over through the boundary layer are discussed. With the aid of flow parameters, the flow phenomenon has been described, and the impact of these parameters on the temperature, concentration, and velocity field has been investigated. The findings from various flow entities have been qualitatively discussed and graphically displayed.

2. Formulation of problems and governing equation

Consider a viscous, physically conductive, incompressible fluid that is being exposed to radiation in a vertical plate-supported MHD free convection flow. The starting point of a coordinate system where $\mathcal{X}-axis$ runs up the plate and $\mathcal{Y}-axis$ is perpendicular to the plate. The temperatures of the inside and outside of the plate are $\mathcal{T}_w$ and $\mathcal{T}_\infty$ respectively. As shown in Fig. 1, a uniform magnetic field $\overline{B}=(0,B_0,0)$ it is usually applied to the board knowind that the magnetic field will be weak as long as B_0 it is kept constant. Unsteady equations of heat, flow, mass, and heat transfer on a vertical plate in the presence of a magnetic field and thermal radiation, together with terms of boundary are shown below:

The two-dimensional free convection fluid flow and heat transfer in the model are described by the

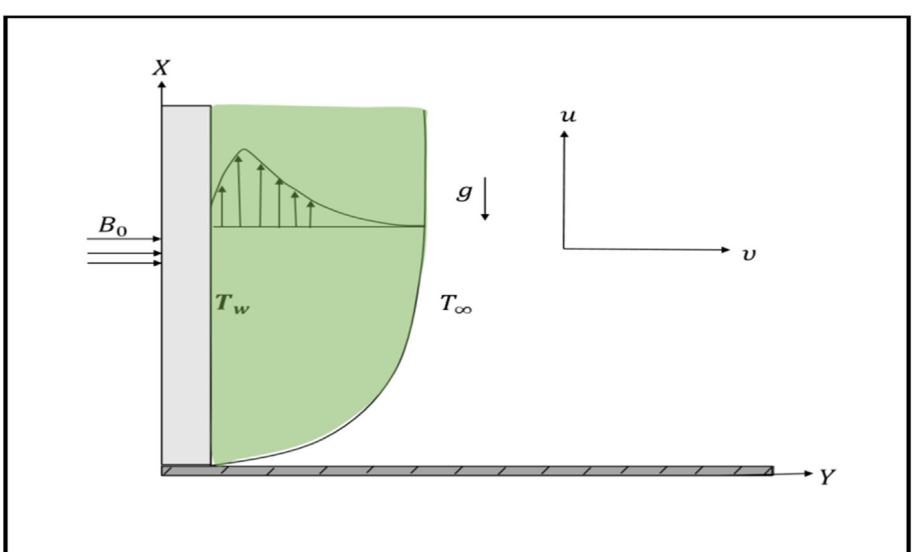

Fig. 1. Mathematical model.

following equations for continuity, Navier−Stokes, and energy:

$$\frac{\partial \mathcal{U}}{\partial \S}+\frac{\partial \mathcal{V}}{\partial y}=0 \tag{1}$$

$$\frac{\partial \mathcal{U}}{\partial t}+\mathcal{U}\frac{\partial \mathcal{U}}{\partial x}+\mathcal{V}\frac{\partial \mathcal{V}}{\partial y}=\nu\left(\frac{\partial^2 \mathcal{U}}{\partial y^2}\right)+\}\beta(\mathcal{T}-\mathcal{T}_\infty)-\frac{\sigma B_0^2}{\rho}\mathcal{U} \tag{2}$$

$$\frac{\partial \mathcal{T}}{\partial t}+\mathcal{U}\frac{\partial \mathcal{T}}{\partial x}+\mathcal{V}\frac{\partial \mathcal{T}}{\partial y}=\frac{\mathcal{K}}{\rho C_p}\left(\frac{\partial^2 \mathcal{T}}{\partial y^2}\right)-\frac{1}{\rho C_p}\left(\frac{\partial \amalg_r}{\partial y}\right)-\frac{\nu}{C_p}\left(\frac{\partial \mathcal{U}}{\partial y}\right)^2 \tag{3}$$

The relevant boundary conditions for temperature and velocity are as follows:

$$\left.\begin{array}{ll}\mathcal{U}=\mathcal{U}_0, \mathcal{V}=0, \mathcal{T}=\mathcal{T}_\infty & at\ y=0\\ \mathcal{U}\to 0, \mathcal{T}\to\mathcal{T}_\infty & at\ y\to\infty\end{array}\right\} \tag{4}$$

Where ν is kinetic instability, $\}$ is gravitationally accelerating, β dilation volumetric factor, $\mathcal{T}$ is the temperature of the fluid inside the thermal, $\mathcal{T}_\infty$ is the heat of the free flow, σ denoted as an electrically conductive, B_0 is the field of magnetism, ρ is the density of the fluid, $\mathcal{K}$ is the permeability of the medium, C_p is the temperature at constant prrssure, $\mathcal{U}_0$ represent the uniform velocity of the fluid, and $\mathcal{T}_w$ is the temperature.

The radiative heat flow for an optically thick fluid should be evaluated using the Roseland approximations, as shown in [17].

$$\amalg_r=\left(\frac{-4\sigma^*}{3k_1}\right)\frac{\partial \mathcal{T}^4}{\partial y} \tag{5}$$

The fixed of Stefan−Boltzmann is σ^*, while k_1 represents the typical absorption factor. The Roseland thermal radiation hypothesis predicts that the temperature differential within the flow will be very modest. $\mathcal{T}^4$ can be generally estimated as follows using Taylor's series: [18].

$$\mathcal{T}^4=4\mathcal{T}_w^3\mathcal{T}-3\mathcal{T}_w^4 \tag{6}$$

Equation (3) and Equation (6) combine to form the following equation (7)

$$\frac{\partial \mathcal{T}}{\partial t}+\mathcal{U}\frac{\partial \mathcal{T}}{\partial x}+\mathcal{V}\frac{\partial \mathcal{T}}{\partial y}=\left(\frac{\mathcal{K}}{\rho C_p}+\frac{16\sigma^*\mathcal{T}_w^3}{3k_1\rho C_p}\right)\left(\frac{\partial^2 \mathcal{T}}{\partial y^2}\right)-\frac{\nu}{C_p}\left(\frac{\partial \mathcal{U}}{\partial y}\right)^2 \tag{7}$$

3. Mathematical formulation

With the use of normal transformations, a non-dimensional system was produced from a collection of boundary-constrained partial differential equations [13].

$$\left.\begin{array}{l}\mathcal{U}=\mathcal{U}_0\overline{\mathcal{U}}, \mathcal{V}=\mathcal{U}_0\overline{\mathcal{V}}, \overline{\mathcal{X}}=\dfrac{\mathcal{X}\mathcal{U}_0}{\nu}, \overline{\mathcal{Y}}=\dfrac{\mathcal{Y}\mathcal{U}_0}{\nu},\\ \eta=\dfrac{t\mathcal{U}_0^2}{\nu}, \overline{\mathcal{T}}=\dfrac{\mathcal{T}-\mathcal{T}_\infty}{\mathcal{T}_w-\mathcal{T}_\infty}, M=\dfrac{\nu\sigma B_0^2}{\rho\mathcal{U}_0^2}\\ Gr=\dfrac{\nu g\beta(\mathcal{T}_w-\mathcal{T}_\infty)}{\mathcal{U}_0^3}, R=\dfrac{3^{k_1}\mathcal{K}+16\sigma^*\mathcal{T}_w^3}{3^{k_1}\mu C_p},\\ Ec=\dfrac{\mathcal{U}_0^2}{C_p(\mathcal{T}_w-\mathcal{T}_\infty)}\end{array}\right\} \tag{8}$$

The aforementioned transformation is applied to equations (1), (2) and (7) and appropriate boundary conditions (4) are used to produce the following simplified nonlinear differential equations. Amount of magnetic, The amount of Gasthof, the radiation number, and the Eckert number are each represented by the letters $M, Gr, R\ and\ Ec$ respectively. Such governing equations have these dimensionless forms:

$$\frac{\partial \overline{\mathcal{U}}}{\partial \overline{\mathcal{X}}}+\frac{\partial \overline{\mathcal{V}}}{\partial \overline{\mathcal{Y}}}=0 \tag{9}$$

$$\frac{\partial \overline{\mathcal{U}}}{\partial \eta}+\overline{\mathcal{U}}\frac{\partial \overline{\mathcal{U}}}{\partial \overline{\mathcal{X}}}+\overline{\mathcal{V}}\frac{\partial \overline{\mathcal{U}}}{\partial \overline{\mathcal{Y}}}=\left(\frac{\partial^2 \overline{\mathcal{U}}}{\partial \overline{\mathcal{Y}}^2}\right)+Gr\overline{\mathcal{T}}-M\overline{\mathcal{U}} \tag{10}$$

$$\frac{\partial \overline{\mathcal{T}}}{\partial \eta}+\overline{\mathcal{U}}\frac{\partial \overline{\mathcal{T}}}{\partial \overline{\mathcal{X}}}+\overline{\mathcal{V}}\frac{\partial \overline{\mathcal{T}}}{\partial \overline{\mathcal{Y}}}=R\left(\frac{\partial^2 \overline{\mathcal{T}}}{\partial \overline{\mathcal{Y}}^2}\right)+Ec\left(\frac{\partial \overline{\mathcal{U}}}{\partial \overline{\mathcal{Y}}}\right)^2 \tag{11}$$

terms defining boundaries:

$$\left.\begin{array}{ll}\overline{\mathcal{U}}=1, \overline{\mathcal{V}}=0, \overline{\mathcal{T}}=1 & at\ \ \overline{\mathcal{Y}}=0\\ \overline{\mathcal{U}}=0, \overline{\mathcal{T}}=0 & at\ \ \overline{\mathcal{Y}}\to\infty\end{array}\right\} \tag{12}$$

4. Numerical solution

The concept behind this approach is based on discretizing equations 9−12 using a finite difference method with recurrent iterations in time. To overcome the double vibration equation (10) and energy equation (11) and initial conditions (12), we try to use the numerical simulation for $-L\le\overline{\mathcal{X}}\le L$ and $-H\le\overline{\mathcal{Y}}\le H$, where L, H are the incidental random length of the calculational field between $\overline{\mathcal{X}}$ and $\overline{\mathcal{Y}}$ direaction. As previously mentioned, the finite difference method is used to solve the central equation of the movement and energy equations 10 and 11. To discretize the domain above in to $N+1$ points in $\overline{\mathcal{X}}$-direction and $M+1$ in $\overline{\mathcal{Y}}$-direction, we use:

$$\overline{\mathcal{X}}i = -L + (i-1)\Delta\overline{\mathcal{X}}, i = 1, \ldots, N+1, \overline{\mathcal{Y}}j = -H + (j-1)\Delta\overline{\mathcal{Y}}, j = 1, \ldots, M+1$$

Where $\Delta\overline{\mathcal{X}} = \frac{2L}{N}$ and $\Delta\overline{\mathcal{Y}} = \frac{2H}{M}$. Consider the forward and backward finite difference methods that are used to discretize the main equation in this paper [19].

$$\frac{\overline{\mathcal{U}}_{i,j} - \overline{\mathcal{U}}_{i-1,j}}{\Delta\overline{\mathcal{X}}} + \frac{\overline{\mathcal{V}}_{i,j} - \overline{\mathcal{V}}_{i,j-1}}{\Delta\overline{\mathcal{Y}}} = 0 \tag{13}$$

$$\overline{\mathcal{U}'}_{i,j} = \overline{\mathcal{U}}_{i,j} + \Delta\eta\left(-\overline{\mathcal{U}}_{i,j}\frac{\overline{\mathcal{U}}_{i,j} - \overline{\mathcal{U}}_{i-1,j}}{\Delta\overline{\mathcal{X}}} - \overline{\mathcal{V}}_{i,j}\frac{\overline{\mathcal{U}}_{i,j+1} - \overline{\mathcal{U}}_{i,j}}{\Delta\overline{\mathcal{Y}}} + \ldots + \frac{\overline{\mathcal{U}}_{i,j+1} - 2\overline{\mathcal{U}}_{i,j} + \overline{\mathcal{U}}_{i,j-1}}{(\Delta\overline{\mathcal{Y}})^2} + Gr\overline{\mathcal{T}}_{i,j} - M\overline{\mathcal{U}}_{i,j}\right) \tag{14}$$

$$\overline{\mathcal{T}'}_{i,j} = \overline{\mathcal{T}}_{i,j} + \Delta\eta\left(-\overline{\mathcal{U}}_{i,j}\frac{\overline{\mathcal{T}}_{i,j} - \overline{\mathcal{T}}_{i-1,j}}{\Delta\overline{\mathcal{X}}} - \overline{\mathcal{V}}_{i,j}\frac{\overline{\mathcal{T}}_{i,j+1} - \overline{\mathcal{T}}_{i,j}}{\Delta\overline{\mathcal{Y}}} + R\left(\frac{\overline{\mathcal{T}}_{i,j+1} - 2\overline{\mathcal{T}}_{i,j} + \overline{\mathcal{T}}_{i,j-1}}{(\Delta\overline{\mathcal{Y}})^2}\right) + +Ec\left(\frac{\overline{\mathcal{U}}_{i,j+1} - \overline{\mathcal{U}}_{i,j}}{\Delta\overline{\mathcal{Y}}}\right)^2\right) \tag{15}$$

Where

$$\frac{\partial\overline{\mathcal{U}}}{\partial\overline{\mathcal{X}}} = \frac{\overline{\mathcal{U}}_{i,j} - \overline{\mathcal{U}}_{i-1,j}}{\Delta\overline{\mathcal{X}}}, \frac{\partial\overline{\mathcal{V}}}{\partial\overline{\mathcal{Y}}} = \frac{\overline{\mathcal{V}}_{i,j} - \overline{\mathcal{V}}_{i,j-1}}{\Delta\overline{\mathcal{Y}}}, \frac{\partial\overline{\mathcal{U}}}{\partial\eta} = \frac{\overline{\mathcal{U}'}_{i,j} - \overline{\mathcal{U}}_{i,j}}{\Delta\eta}$$

$$\frac{\partial^2\overline{\mathcal{U}}}{\partial\overline{\mathcal{Y}}^2} = \frac{\overline{\mathcal{U}}_{i,j+1} - 2\overline{\mathcal{U}}_{i,j} + \overline{\mathcal{U}}_{i,j-1}}{(\Delta\overline{\mathcal{Y}})^2}, \frac{\partial\overline{\mathcal{T}}}{\partial\overline{\mathcal{X}}} = \frac{\overline{\mathcal{T}}_{i,j} - \overline{\mathcal{T}}_{i-1,j}}{\Delta\overline{\mathcal{X}}}$$

$$\frac{\partial\overline{\mathcal{T}}}{\partial\overline{\mathcal{Y}}} = \frac{\overline{\mathcal{T}}_{i,j+1} - \overline{\mathcal{T}}_{i,j}}{\Delta\overline{\mathcal{Y}}}, \frac{\partial\overline{\mathcal{T}}}{\partial\eta} = \frac{\overline{\mathcal{T}'}_{i,j} - \overline{\mathcal{T}}_{i,j}}{\Delta\eta}, \frac{\partial^2\overline{\mathcal{T}}}{\partial\overline{\mathcal{Y}}^2} = \frac{\overline{\mathcal{T}}_{i,j+1} - 2\overline{\mathcal{T}}_{i,j} + \overline{\mathcal{T}}_{i,j-1}}{(\Delta\overline{\mathcal{Y}})^2}$$

$$\frac{\partial\overline{\mathcal{U}}}{\partial\overline{\mathcal{Y}}} = \frac{\overline{\mathcal{U}}_{i,j+1} - \overline{\mathcal{U}}_{i,j}}{\Delta\overline{\mathcal{Y}}}$$

Initial and constraints of limits for finite difference methods as the following

$$\left.\begin{aligned} \overline{\mathcal{U}}^n_{i,0} = 1, \overline{\mathcal{V}}^n_{i,0} = 0, \overline{\mathcal{T}}^n_{i,0} = 1 \\ \overline{\mathcal{U}}^n_{i,L} = 0, \overline{\mathcal{T}}^n_{i,L} = 0 \end{aligned}\right\} \tag{16}$$

Where $\overline{\mathcal{T}}$ stands for temperature and $L \to \infty$, i and j are grid points with corresponding $\overline{\mathcal{X}}$ and $\overline{\mathcal{Y}}$ coordinates.

5. Results and discussions

The effects of various parameters on the temporal material amounts are computed, illustrated in Fig. 2−9, and thoroughly concerned in order to gain a physical interpretation of the issue. Figure 2 shows the outcome of the Gratshof numeral. For a steady magnetic number, it is seen that the velocity domain develops as the gradient number increases. We can also notice that the velocity increases as we move away from the plate before beginning to decrease. Figure 3 depicts the magnetic number's impact. Additionally, we see that the momentum speed

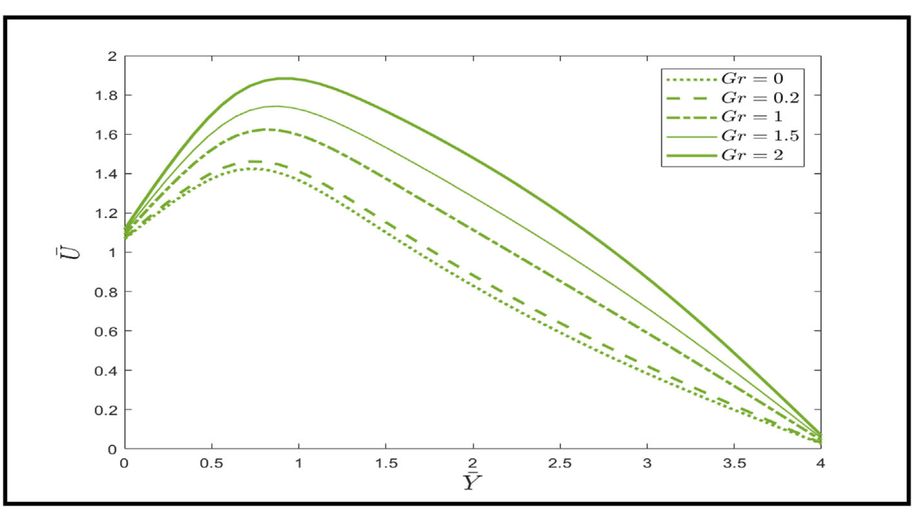

Fig. 2. Speed profile $\overline{U}$ for several values of Gr.

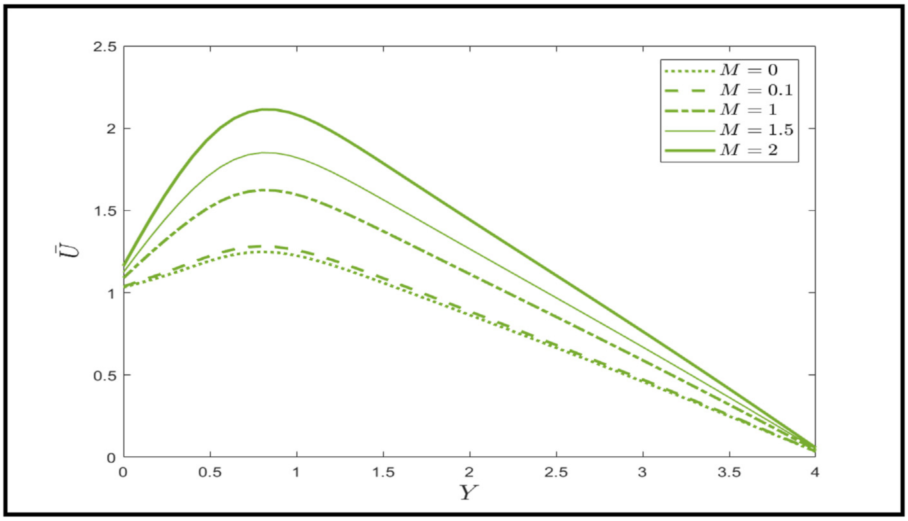

Fig. 3. Velocity profile $\overline{U}$ for various value of M.

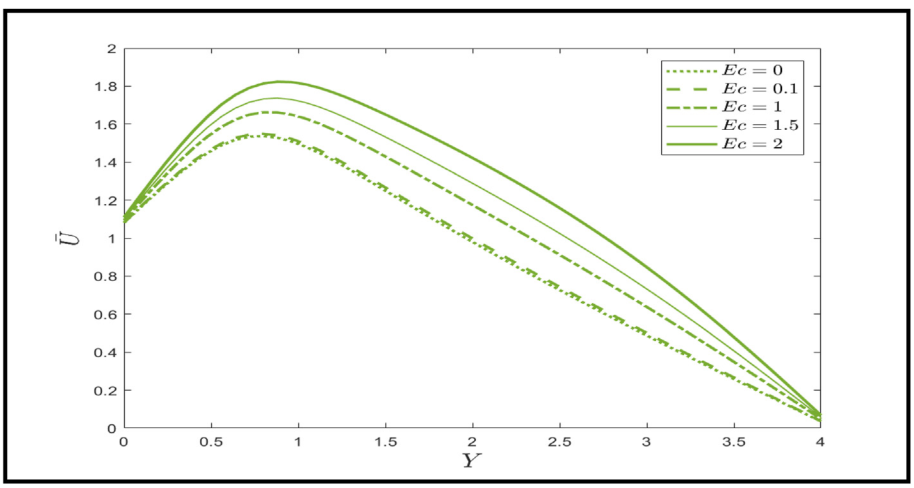

Fig. 4. Velocity profile $\overline{U}$ for several value of Ec.

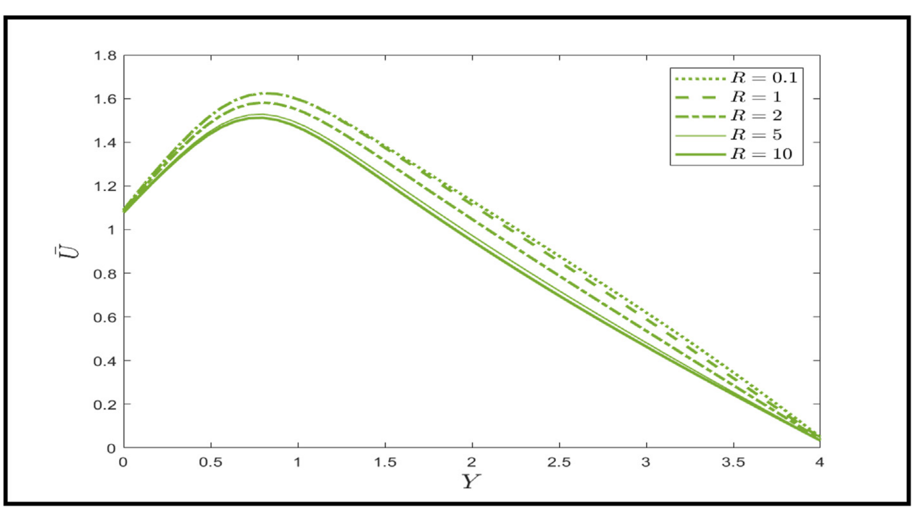

Fig. 5. Velocity profile $\overline{U}$ for different value of R.

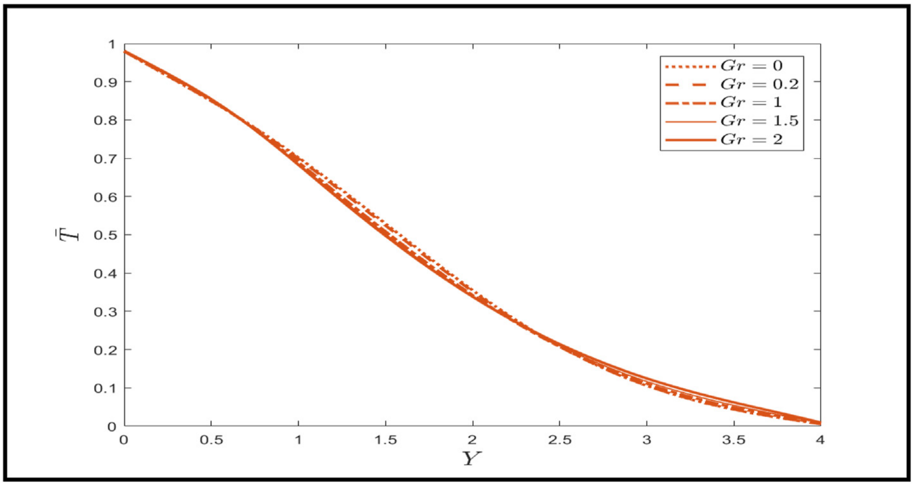

Fig. 6. Temperature profile $\overline{T}$ *for various value of Gr.*

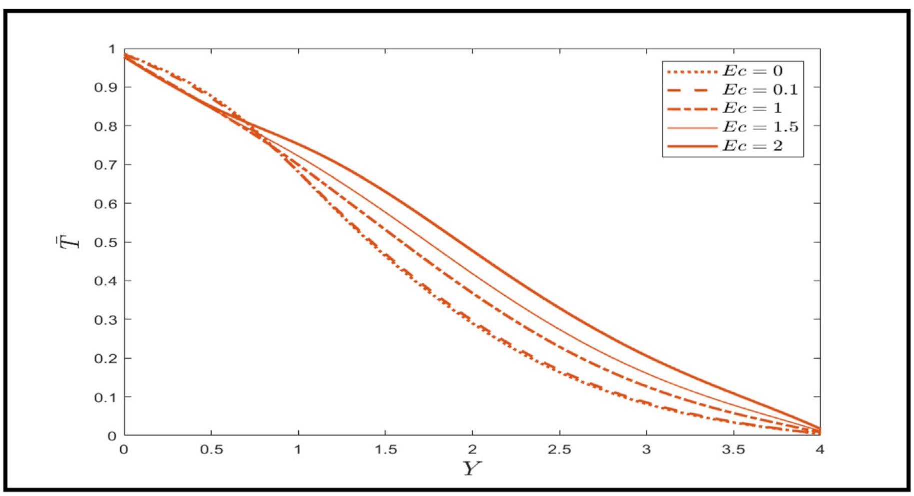

Fig. 7. Temperature profile $\overline{T}$ *for different value of Ec.*

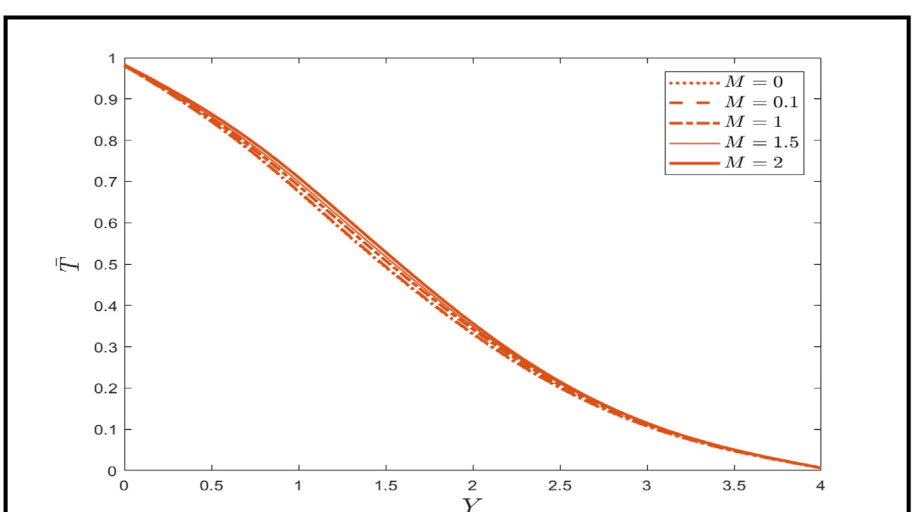

Fig. 8. Temperature profile $\overline{T}$ *for different value of M.*

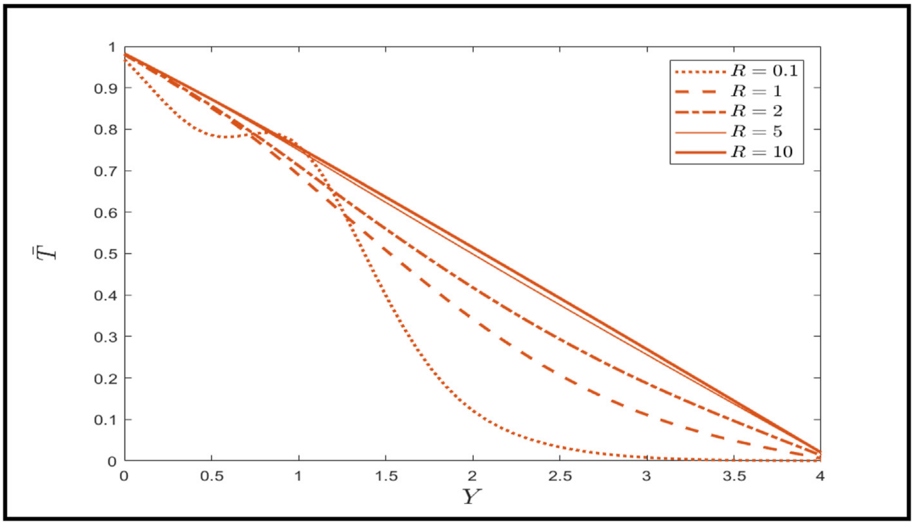

Fig. 9. Temperature profile $\overline{T}$ for different value of R.

grows as we push out from the plate before it starts to fall. The impact of the Eckert number on the velocity field is shown in Fig. 4, where an increase in the Eckert number leads to an acceleration of the speed area; however, the pattern seems to have modified as we walk away from the plate, and the velocity field seems to conduct differently in each of these points. Figure 5 illustrates how the radiation parameter affects the speed field. An increase in the radiation parameter yields a decrease in the velocity field. Figures 6 and 8 show the temperature shapes for various slope and magnetic numbers. Thus, it is exhibited that the Gratshof and Magnetic numbers have a small effect on temperatures. The temperature field is influenced by the Eckert number, as illustrated in Fig. 7. An increase in the Eckert number causes the temperature field to accelerate. The association between the temperature area and the thermal radiation parameter is shown in Fig. 9, where the temperature field advances as the thermal radiation parameter does.

6. Conclusions

The purpose of this work is to examine MHD free convection flow over a perpendicular scale while thermal radiation and magnetic forces are present. The finite difference method (17) is used utilized to numerically solve the initial values problems the initial value problems resulting from the set of partial differential equations (14)−(16), all of which involve boundary conditions. The effects of the non-dimensional Gratshof parameter Gr, the magnetic number M, the Eckert number Ec, and the radiation number 0 are shown in Figs. 2−9.

Acknowledgements

The authors thank the University of Mosul's College of Education for Pure Science for its assistance in raising the project's caliber.

Funding

Self-funding.

References

[1] Joseph K, Peter A, Asie PE, Usman S. The unsteady MHD free convective two immiscible fluid flows in a horizontal channel with heat and mass transfer. Int J Math Comp Res 2015;3(5):954−72.
[2] Kumar S, Singh Ch. Heat transfer and fluid flow characteristic of blood flow in multi- stenosis artery with effect of magnetic field. Indian J Biomech: Special Issue 2009:186−90 (NCBM 7-8 March).
[3] Seethamahalakshmi, Ramana Reddyr GV, Prasad BDCN. Unsteady MHD free convection flow and mass transfer near a moving vertical plate in the presence of thermal radiation. Adv Appl Sci Res 2011;2(6):261−9.
[4] Zhang Jing-Kui, Li Ben-Wen, Chen Yuan-Yuan. Hall effects on natural convection of participating MHD with thermal radiation in a cavity. Int J Heat Mass Tran 2013;66: 838−43.
[5] Narahari M, Tippa Sowmya, Pendyala Rajashekhar. Unsteady magneto hydrodynamic free convection flow of a radiative fluid past an infinite vertical plate with constant heat and mass flux. Appl Mech Mater 2014;465−466:149−54.
[6] Namdeppanavar MM, Shilpa JM. Stagnation point flow of non- Newtonian fluid and heat transfer over stretching/shrinking sheet. Chem Process Eng Res 2016;46:27−34.
[7] Ibrahim M, Suneetha K. Effects of thermal diffusion and chemical reaction on MHD transient free convection flow past a porous vertical plate with radiation, temperature gradient dependent heat source in slip flow regime. J Comput Appl Res Mech Eng 2016;5(2):83−95.
[8] Kumari K, Goyal M. Heat and mass transfer flow of MHD viscous dissipative fluid in a channel with a stretching and porous plate. Int J Appl Math Inform Sci Lett 2017;5:81−7.

[9] El-Amin MF, Khaled U, Beroual A. Numerical study of effects of Soret-Dufour, Hall, radiation and chemical. J Creat Res Thought (IJCRT) 2018;6(1).
[10] El-Amin MF, Khaled U, Beroual A. Numerical study of the magnetic field effect on ferromagnetic fluid flow and heat transfer in a square porous cavity. Energies 2018;11(11):3235. https://doi.org/10.3390/en11113235.
[11] Rahman A, Wenqian X, Kunhang L, Hua-Shu D, Boo Cheong K, Jie M. Influence of magnetic force on the flow stability in a rectangular duct. Adv Appl Math Mech 2019; 11(1):24−37.
[12] Hammodat A, Al-Bairaqdar OT, Hammodat AT. Numerical solution of energy equation in porous channels under effects of radiation field. Iraqi J Sci 2021;62(10):3620−33. https://doi.org/10.24996/ijs.2021.62.10.20.
[13] Ullah M, Tarammim A, Uddin M. A study of two dimensional unsteady MHD free convection flow over a vertical plate in the presence of radiation. Open J Fluid Dynam 2021;11:20−31.
[14] Nagaraju V, Uthayakumar C. Aligned magnetic field and thermal radiation effects on unsteady MHD flow an inclined porous plate with chemical reaction and heat source: finite difference technique. J Math Control Sci Appl 2021;17(1): 145−61.
[15] Adeshina T, Joel C. Effect of the variable electrical conductivity on the thermal stability of the MHD reactive squeezed fluid flow through a channel by a spectral collocation approach. Part Diff Eq Appl Math 2022;5. https://doi.org/10.1016/j.padiff.2021.100256.
[16] Bodoloi R, Ahmed N. MHD free convection from a semi-infinite vertical porous plate with diffusion-thermo effect. Plat Open Access J 2022;12(6):7685−95.
[17] Brewster M. Thermal radiative transfer properties. New York: John Wiley and Sons; 1972.
[18] Bhattacharyya K. MHD stagnation-point flow of Casson fluid and heat transfer over a stretching sheet with thermal radiation. J Thermodyn 2013. https://doi.org/10.1155/2013/169674. Available Article ID 169674.
[19] Ahmed K. Advantages and disadvantages of using MATLAB/Ode45 for solving differential equations in engineering applications. Int J Eng 2013;7(1):25−31.